nature neuroscience

Hypothalamic CRFR1 is essential for HPA axis regulation following chronic stress

Assaf Ramot[1,2], Zhiying Jiang[3], Jin-Bin Tian[4], Tali Nahum[1,2], Yael Kuperman[5], Nicholas Justice[3] & Alon Chen[1,2]

The hypothalamic–pituitary–adrenal axis is a pivotal component of an organism's response to stressful challenges, and dysfunction of this neuroendocrine axis is associated with a variety of physiological and psychological pathologies. We found that corticotropin-releasing factor type 1 receptor within the paraventricular nucleus of the hypothalamus is an important central component of hypothalamic–pituitary–adrenal axis regulation that prepares the organism for successive exposure to stressful stimuli.

Exposure to stressful challenges modifies the activity of neuronal circuits associated with a variety of central functions, which collectively serve to adaptively respond to the stressful situation. The hypothalamic–pituitary–adrenal (HPA) axis is a pivotal component of this stress response[1]. Dysfunction of the HPA axis is implicated in the etiology of various physiological[2] and psychological pathologies[3], and therefore mechanisms regulating HPA axis function are highly relevant in the treatment of stress-related disease. The neuropeptide corticotropin-releasing factor (CRF), expressed in and secreted from parvocellular neurons of the paraventricular nucleus (PVN) of the hypothalamus, represents the final common step in the integration of the neuroendocrine stress response in the brain[4]. CRF plays an essential and well-established role in the regulation of the HPA axis both under 'basal' and stressful conditions[5]. Upon reaching the anterior pituitary, CRF stimulates adrenocorticotropic hormone release into the peripheral blood stream. In turn, adrenocorticotropic hormone initiates the secretion of glucocorticoids (GCs; corticosterone (CORT) in rodents and cortisol in humans) from the adrenal cortex[6]. GCs, via the glucocorticoid and mineralocorticoid receptors (GR and MR), are fundamental peripheral and central transcriptional regulators in the response to stressful challenges. In addition, they provide negative feedback at multiple levels of the HPA axis[7]. CRF induces its effects by activating two receptors: CRF receptor type 1 (CRFR1)[8] and CRF receptor type 2 (CRFR2)[9]. CRFR1 is widely expressed in the mammalian brain and pituitary and is required for HPA axis activation[10–12].

Here we describe and characterize the physiological role of a distinct population of PVN CRFR1-positive (CRFR1$^+$) neurons that are in close proximity to HPA axis-initiating PVN CRF neurons (**Fig. 1a**). Since no reliable antibody for CRFR1 (ref. 13) is currently available, we used a validated transgenic mouse model that expresses GFP specifically in CRFR1$^+$ neurons (*CRFR1^{GFP}*; ref. 10) to characterize the molecular and cellular phenotype of PVN CRFR1$^+$ neurons. We found that PVN CRFR1$^+$ neurons represented a distinct neuronal population residing in the PVN that did not colocalize with classical PVN markers such as CRF, arginine vasopressin, oxytocin or other parvocellular neurosecretory neuronal populations (**Fig. 1a–d**, **Supplementary Fig. 1a** and **Supplementary Video 1**). Single-cell reverse-transcription-PCR of PVN CRFR1-GFP$^+$ neurons revealed that more than 90% (11 of 12) of these neurons expressed mRNA for GABA-synthesizing enzymes GAD, suggesting a GABAergic phenotype (**Supplementary Fig. 1c**).

Bath perfusion of CRF (10 nM) robustly increased the firing rate in 5 of 6 CRFR1-GFP$^+$ neurons in the PVN (to 382.04 ± 35.24% of baseline, $P = 0.001$, $n = 6$). Preincubation with Astressin[14], a CRF-receptor antagonist, completely blocked the CRF-induced neuronal excitability (99.55 ± 5.08% of baseline, $n = 6$; $P = 0.93$ compared to CRF alone, $n = 6$). In addition, the CRF-induced increase in firing rate was not affected by fast synaptic blockers CNQX (20 μM), D-AP5 (30 μM) or picrotoxin (100 μM)—firing increased to 738.51 ± 152.83% of baseline, $P = 0.009$, $n = 6$; not significantly different from the effect of CRF—which is consistent with CRF acting directly on CRFR1 neurons (**Fig. 1e,f**). We further confirmed that PVN CRF fibers are adjacent to PVN CRFR1$^+$ neurons by injecting a Cre-dependent mCherry virus into the PVN of *CRF^{Cre}* mice[15], which had been crossbred with *CRFR1^{GFP}* mice (*CRF^{Cre}* × *CRFR1^{GFP}*), conditionally tagging PVN CRF$^+$ neurons red. Red fluorescent puncta can be seen contacting green fluorescent CRFR1$^+$ cells, suggesting that cell–cell contacts are made between these neuronal populations (**Supplementary Fig. 1b** and **Supplementary Video 2**). To determine whether or not cell contacts between CRF$^+$ and CRFR1$^+$ neurons form functional synapses, we injected a Cre-dependent channelrhodopsin-expressing virus (AAV-EF1α-DIO-hChR2(H134R)-p2A-Ruby) into the PVN of *CRF^{Cre}* × *CRFR1^{GFP}* mice to optically drive CRF neuronal firing (**Fig. 1g–j**). Optical activation of PVN CRF$^+$ neurons evoked excitatory postsynaptic potentials (EPSPs) in 3 of 14 neurons (average amplitude, 80.82 pA; delay, 4.5 ms), and in neurons without evoked EPSPs, 7 of 11 neurons showed increased firing frequency in response to a 1–3 min laser train (1 Hz, 5 ms, 5–6 mW), from 0.11 ± 0.06 Hz to 1.56 ± 2.28 Hz ($n = 7$, $P = 0.02$, signed-rank test; **Fig. 1i,j**). These data indicate not only that fast synaptic contacts were present between CRF$^+$ and CRFR1$^+$ neurons but also that release of CRF mediates signaling between these populations in the absence of fast synaptic contacts.

Since the PVN is a hub for integrating the neuroendocrine response to stressful challenges, we hypothesized that PVN CRFR1 expression might be regulated, similarly to PVN CRF expression, by GCs. To test this hypothesis, we took advantage of the well-established phenotype of CRFR1-deficient (*CRFR1$^{-/-}$*) mice. These mice have persistently low levels of circulating CORT and blunted HPA axis activity, due to the lack of response to CRF in the anterior pituitary[16]. To elucidate whether GCs

[1]Department of Neurobiology, Weizmann Institute of Science, Rehovot, Israel. [2]Department of Stress Neurobiology and Neurogenetics, Max Planck Institute of Psychiatry, Munich, Germany. [3]Institute of Molecular Medicine, University of Texas Health Sciences Center, Houston, Texas, USA. [4]Department of Integrative Biology and Pharmacology, University of Texas Health Sciences Center, Houston, Texas, USA. [5]Department of Veterinary Resources, Weizmann Institute of Science, Rehovot, Israel. Correspondence should be addressed to A.C. (Alon.Chen@weizmann.ac.il) or N.J. (Nicholas.J.Justice@uth.tmc.edu).

Received 27 September 2016; accepted 2 January 2017; published online 30 January 2017; doi:10.1038/nn.4491

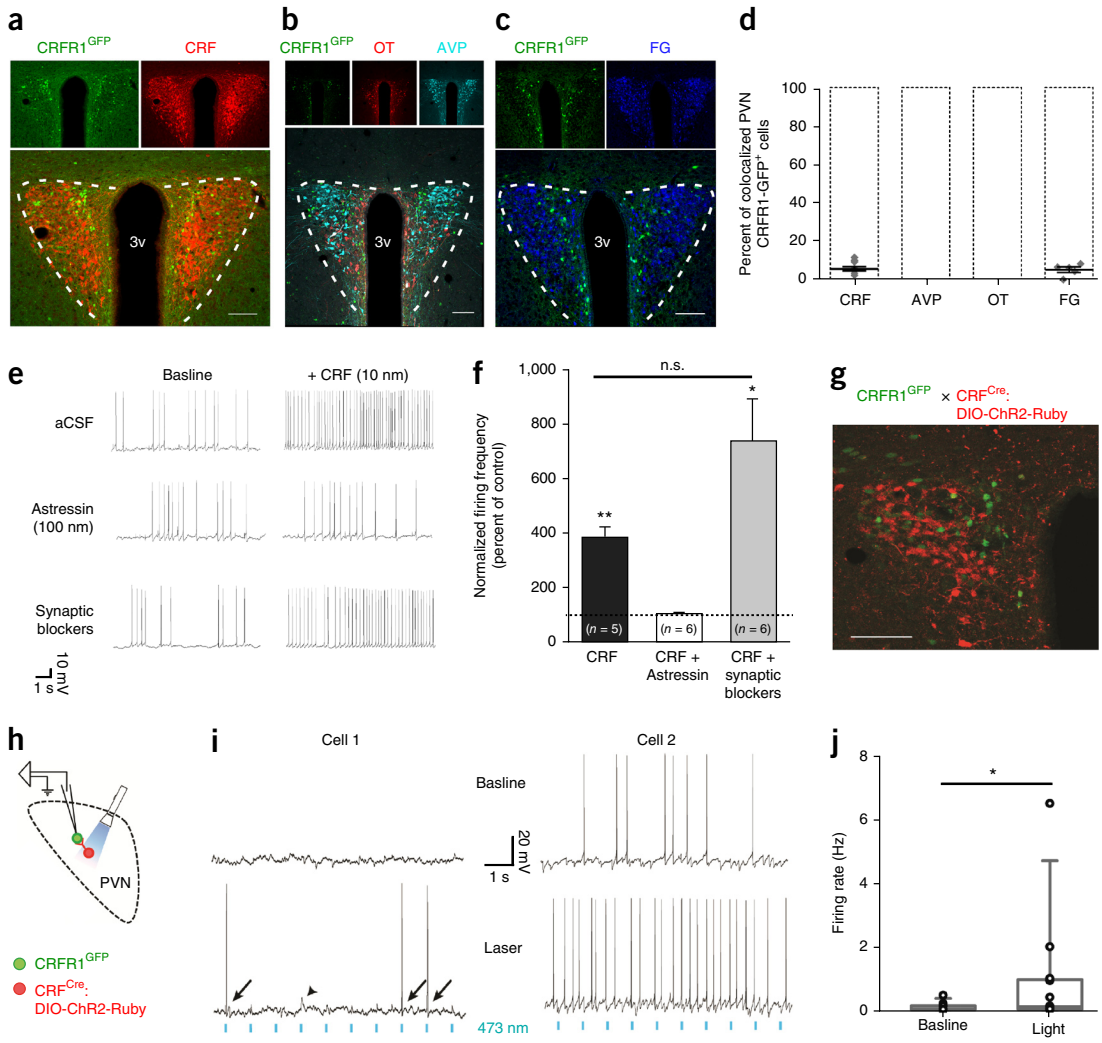

Figure 1 CRFR1+ neurons represent a distinct neuronal population residing in the PVN. (**a**–**c**) Brain coronal sections obtained from *CRFR1*^{GFP} mice immunostained for (**a**) CRF, (**b**) oxytocin (OT) and arginine vasopressin (AVP) and (**c**) retrogradely traced with peripheral Fluoro-Gold (FG). 3v, third ventricle. Magnification, 20×; scale bars, 100 µm. (**d**) Summary of colocalized PVN CRFR1-GFP+ neurons. Only a small percentage (±5%) of neurons are positive for CRF or FG, and no CRFR1-GFP+ neurons express AVP or OT (n = 6, 4 and 5 mice, respectively; each data point represents one PVN slice). (**e**) Representative traces from whole-cell patch-clamp recordings showing that bath application of CRF (10 nM) increases action potential firing of CRFR1+ neurons in the PVN (P = 0.001; top traces). Excitation is blocked by the CRF receptor antagonist Astressin (100 nM; P = 0.93; middle traces) but not by glutamate- or GABA-receptor antagonists CNQX (20 µM), AP-5 (30 µM) and picrotoxin (100 µM) (P = 0.009 compared to baseline; not significantly different from CRF, P = 0.068; bottom traces). aCSF, artificial cerebrospinal fluid. (**f**) Summary histogram of mean normalized action potential firing in response to bath application of CRF (10 nM). Dashed line indicates baseline (100%); *P = 0.009 and **P = 0.001 compared to baseline. Student's t-test. (**g**–**j**) PVN CRFR1+ neurons are excited by optical activation of neighboring CRF neurons. (**g**) *CRF*^{Cre} × *CRFR1*^{GFP} mice were injected in the PVN with adeno-associated virus (AAV) encoding Cre-releasable ChR2-Ruby. ChR2-Ruby+ CRF neurons are located in close proximity to PVN CRFR1-GFP+ neurons. Scale bar, 100 µm. (**h**) Diagram of the experimental setup. (**i**) Representative recordings of CRFR1 neurons in response to optical activation of PVN CRF neurons. Three of 14 cells displayed laser-evoked fast EPSPs time-locked to laser activation (arrows, action potentials; arrowhead, EPSP; cell 1, left); 7 of 11 cells displayed no fast synaptic connections but increased firing when exposed to a laser train (1 Hz, 5 ms, 1–3 min; cell 2, right). (**j**) Quantification of CRFR1+ neuron responses to optical activation of PVN CRF+ neurons in the absence of fast synapses (n = 7, *P = 0.02, signed-rank test). All values for all figures are presented as mean ± s.e.m.

may affect PVN CRFR1 expression, we crossbred *CRFR1*^{GFP} mice with *CRFR1*$^{-/-}$ mice. A CRFR1-GFP signal was not detectable within the borders of the PVN of *CRFR1*^{GFP} × *CRFR1*$^{-/-}$ mice (**Fig. 2a**). To confirm that this downregulation of CRFR1-GFP signal was indeed due to the absence of GCs in these mice, we injected *CRFR1*^{GFP} × *CRFR1*$^{-/-}$ mice with either dexamethasone (DEX; a corticosteroid receptor agonist) or saline. Seven days later, PVN CRFR1-GFP expression was restored in *CRFR1*^{GFP} × *CRFR1*$^{-/-}$ mice that were injected with DEX, whereas GFP was still undetectable in *CRFR1*^{GFP} × *CRFR1*$^{-/-}$ mice injected with saline (**Fig. 2a**,**b**). As *CRFR1*$^{-/-}$ mice might have other deficits in addition to low levels of circulating GCs, we further studied the regulation of PVN CRFR1-GFP expression using adrenalectomized *CRFR1*^{GFP} mice (*CRFR1*$^{GFP:ADX}$). Similarly, *CRFR1*$^{GFP:ADX}$ mice showed a robust reduction in CRFR1-GFP signal in the PVN. Again, when adrenalectomized animals were treated with DEX, PVN CRFR1-GFP expression was restored (**Fig. 2c**,**d**). Hence, unlike CRF, which was negatively regulated by GCs (**Fig. 2a**), PVN CRFR1 was positively regulated by GCs. Notably, this effect was restricted to the PVN, as GFP expression in other brain regions did not change in *CRFR1*$^{GFP:ADX}$ mice treated with DEX compared to *CRFR1*$^{GFP:ADX}$ treated with saline (**Supplementary Fig. 2**).

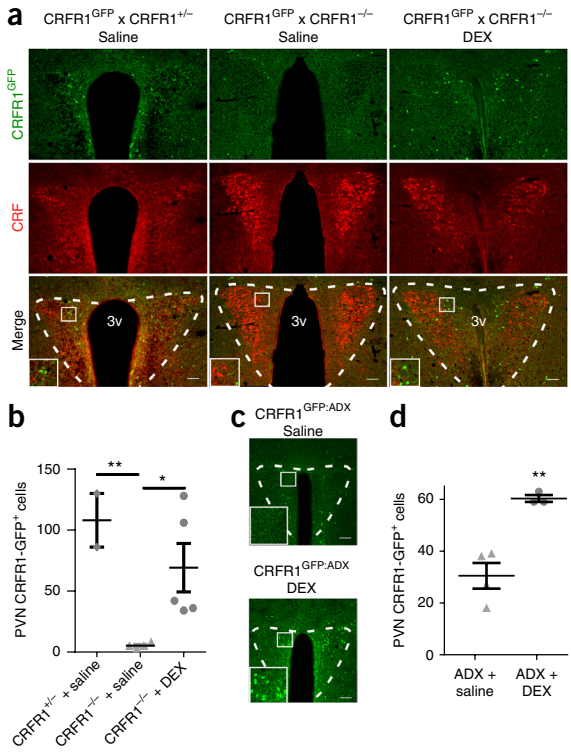

Figure 2 PVN CRFR1 levels are positively regulated by GCs. (**a**) PVN CRFR1-GFP expression is downregulated in *CRFR1*^{GFP} × *CRFR1*$^{-/-}$ mice and restored with DEX treatment. Brain coronal sections obtained from a *CRFR1*^{GFP} × *CRFR1*$^{-/-}$ mouse and immunostained for GFP following treatment with vehicle (middle panel) or DEX (right panel) and compared to *CRFR1*^{GFP} × *CRFR1*$^{+/-}$ mouse treated with saline (left panel). (**b**) Summary of PVN CRFR1-GFP^{+} neurons. PVN CRFR1-GFP expression is significantly lower in the *CRFR1*$^{-/-}$ + saline group compared to the *CRFR1*$^{-/+}$ group and *CRFR1*$^{-/-}$ + DEX group ($F_2 = 7.43$, $P = 0.015$, CRFR1$^{+/-}$ $n = 2$, CRFR1$^{-/-}$ + saline $n = 4$ and CRFR1$^{-/-}$ + DEX $n = 5$ mice per group). (**c**) The downregulation of PVN CRFR1-GFP expression in *CRFR1*$^{GFP:ADX}$ mice is restored by DEX treatment. Brain coronal sections obtained from *CRFR1*$^{GFP:ADX}$ mice, immunostained for GFP 24 h after treatment with saline (upper panel) or DEX (lower panel). (**d**) Summary of PVN CRFR1-GFP^{+} neurons. GFP expression is significantly lower in the *CRFR1*$^{GFP:ADX}$ + saline group compared to the *CRFR1*$^{GFP:ADX}$ + DEX group. ($t_3 = 5.79$, $P = 0.007$, $n = 4$ and 3 mice per group, respectively). All values for all figures are presented as mean ± s.e.m. $^{*}P < 0.05$, $^{**}P < 0.01$. Magnification, 20×; scale bars, 100 µm.

The effects of GCs on PVN CRFR1 neurons was likely directly mediated by affecting CRFR1 transcription via GR, since PVN CRFR1-GFP^{+} neurons coexpressed GRs (**Supplementary Fig. 3a**,**b**).

To elucidate the physiological role of endogenous CRFR1 in the PVN, we established a conditional knockout (cKO) mouse model deficient for CRFR1 specifically within the PVN by crossing *CRFR1*$^{loxP/loxP}$ mice with *Sim1*^{Cre} (ref. 17) mice. To validate the mouse model, we estimated the colocalization between Sim1-Cre^{+} cells and CRFR1-GFP^{+} cells. To this end, we crossbred *Sim1*^{Cre} mice with the *Ai9* reporter mice (conditionally tagging Sim1-Cre^{+} neurons in red)[18] and then with *CRFR1*^{GFP} mice. PVN CRFR1-GFP^{+} cells were highly colocalized with tdTomato^{+} cells in *Sim1*^{Cre} × *Ai9* × *CRFR1*^{GFP} mice (**Fig. 3a**,**b** and **Supplementary Fig. 3c**). To explore the HPA axis function of *CRFR1*$^{PVN\text{-}cKO}$ mice, we measured circulating CORT levels after exposing mice to different stressors. Exposure to acute stressors (restraint, LPS injection or hemorrhage; **Supplementary Fig. 4a–c**), as well as pharmacologically challenging the HPA axis negative feedback (using the DEX suppression test; **Supplementary Fig. 4d**), did not reveal a significant difference in plasma CORT levels between *CRFR1*$^{PVN\text{-}cKO}$ mice and control littermates. This suggests that PVN CRFR1 was not required for the regulation of HPA axis activity under acute stress conditions.

We then explored whether the absence of PVN CRFR1 affected the function of the HPA axis following exposure to chronic stress. Mice were exposed to the chronic social defeat stress (CSDS) protocol[19]. CSDS resulted in typical social avoidance behavior at the end of the protocol in both *CRFR1*$^{PVN\text{-}cKO}$ mice and control littermates (**Supplementary Fig. 5**). However, while basal CORT levels of *CRFR1*$^{PVN\text{-}cKO}$ mice did not differ from control mice before the CSDS exposure (**Fig. 3c**), *CRFR1*$^{PVN\text{-}cKO}$ mice exhibited significantly decreased basal CORT levels 10 d following the termination of the CSDS protocol. (**Fig. 3c**). These results suggest that PVN CFR1 action was essential for HPA axis function following chronic stress. Since we only observed a difference in CORT levels between *CRFR1*$^{PVN\text{-}cKO}$ mice and control littermates following chronic stress, we hypothesize that PVN CRFR1^{+} neurons were recruited specifically during chronic stress exposure. To test this hypothesis, *CRFR1*^{GFP} mice were killed for analysis 90 min after the end of acute social defeat stress (acute SDS) or CSDS. Notably, exposure to acute SDS in mice previously exposed to CSDS resulted in a significantly higher percentage of c-Fos^{+} PVN CRFR1-GFP^{+} neurons, compared to mice exposed to acute SDS only (**Fig. 3d**,**e**). Similarly, while *CRFR1*$^{PVN\text{-}cKO}$ mice showed no differences in anxiety-like behaviors compared to control mice under basal conditions (**Fig. 3f** and **Supplementary Fig. 6**), they did show a robust reduction in anxiety-like behavior in the elevated plus maze test following CSDS (**Fig. 3g**). Notably, this effect was not due to an increase in general locomotor activity in the deficient mice, since dark-phase home-cage locomotion was lower in *CRFR1*$^{PVN\text{-}cKO}$ mice compared to control mice regardless of CSDS exposure (**Supplementary Fig. 7**).

In summary, we show that PVN CRFR1^{+} neurons represent a distinct population of hypothalamic neurons, which are functionally recruited only following prior exposure to chronic stress. While the negative feedback of GCs on PVN CRF expression is a fundamental characteristic of HPA axis regulation, here we demonstrate positive feedback from GCs on PVN CRFR1 expression (**Supplementary Fig. 8a**). In addition, PVN CRFR1 plays a role in modulating HPA axis activity, specifically under chronic stress conditions, by preparing the organism for subsequent exposure to stressful stimuli (**Supplementary Fig. 8b**). Notably, CRFR1 is also expressed in the PVN of humans, where its expression has been found to be elevated in depressed patients[20]. Future studies are needed to explore the involvement of PVN CRFR1 in stress-related neuroendocrine and psychiatric disorders.

METHODS

Methods, including statements of data availability and any associated accession codes and references, are available in the online version of the paper.

Note: Any Supplementary Information and Source Data files are available in the online version of the paper.

ACKNOWLEDGMENTS

We thank N. Nevo for assistance with the adrenalectomy procedure. We thank S. Ovadia and Y. Madar for their devoted assistance with animal care. We thank J. Keverne for professional English editing, formatting and scientific input. A.C. is supported by the Max Planck Society and the Weizmann Institute of Science. This work was supported by an FP7 grant from the European Research Council (260463); a research grant from the Israel Science Foundation (1565/15); research support from Roberto and Renata Ruhman; Bruno and Simone Licht; the Nella and Leon Benoziyo Center for Neurological Diseases; the Henry Chanoch Krenter Institute for Biomedical Imaging and Genomics; the Perlman Family Foundation, founded by Louis L. and Anita M. Perlman;

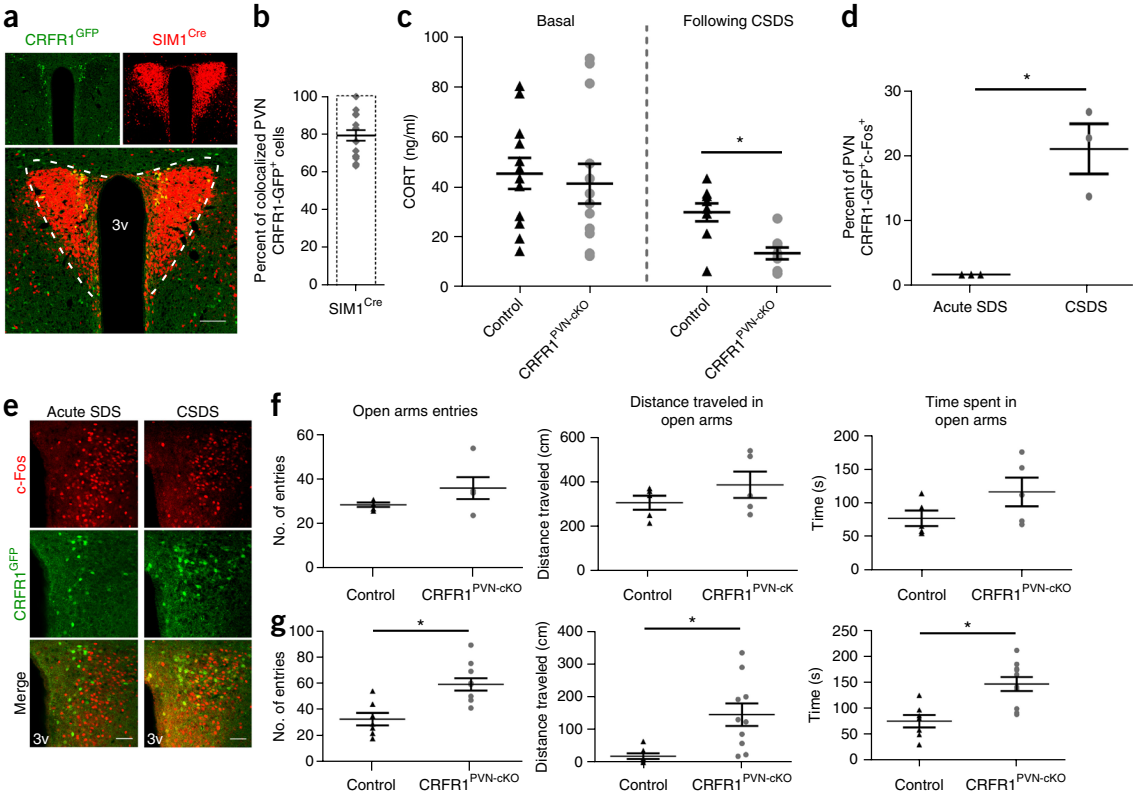

Figure 3 PVN CRFR1 has a neuroendocrine and behavioral role specifically following chronic stress. (**a**) Coronal brain sections taken from *Sim1*^{Cre} × *Ai9* × *CRFR1*^{GFP} mice. Magnification, 20×; scale bar, 100 µm. (**b**) Summary of colocalization of Sim1-Cre and PVN CRFR1-GFP$^+$ neurons showing that 80% of PVN CRFR1-GFP$^+$ neurons coexpress *Cre* (visualized by lox-stop-lox-tdTomato). $n = 2$ mice; each data point represents one PVN slice. (**c**) *CRFR1*$^{PVN\text{-}cKO}$ mice show decreased basal CORT levels following CSDS. Left: no difference was observed between *CRFR1*$^{PVN\text{-}cKO}$ mice and controls in basal morning CORT levels before the beginning of the CSDS protocol ($t_{23} = 4.08$, n.s.). Right: *CRFR1*$^{PVN\text{-}cKO}$ mice show significantly lower levels of morning CORT 10 d after the cessation of the CSDS protocol compared to controls ($t_{17} = 2.94$, $P = 0.009$; $n = 11$ (before CSDS) and 9 (following CSDS) *CRFR1*$^{PVN\text{-}cKO}$ mice and 13 (before CSDS) and 9 (following CSDS) control mice per group, based on independent sample *t*-test). (**d**,**e**) PVN CRFR1-GFP$^+$ neurons are recruited following CSDS but not acute SDS. (**d**) Summary of PVN CRFR1-GFP$^+$ neurons coexpressing the immediate early gene *Fos*. Following CSDS, PVN CRFR1-GFP$^+$ neurons coexpress c-Fos at a significantly higher frequency than following acute SDS ($t_2 = 5.02$, $P = 0.037$). Data presented as mean ± s.e.m.; $n = 3$ mice per group. (**e**) Brain coronal sections obtained from *CRFR1*^{GFP} mice immunostained for c-Fos. *CRFR1*^{GFP} mice were killed for analysis 90 min after the end of either acute SDS or CSDS. Magnification, 20×; scale bars, 100 µm. (**f**,**g**) *CRFR1*$^{PVN\text{-}cKO}$ mice show less anxiety-like behavior following CSDS. (**f**) No difference was observed between *CRFR1*$^{PVN\text{-}cKO}$ mice and controls in elevated-plus maze open arms visits (left; $t_8 = 1.48$, n.s.), open arms distance traveled (middle; $t_6 = 1.2$, n.s.) or time spent in the open arms (right; $t_8 = 1.6$, n.s.). Data presented as mean ± s.e.m.; $n = 5$ mice per group. (**g**) Following chronic SDS, *CRFR1*$^{PVN\text{-}cKO}$ mice enter the open arms more frequently (left; $t_{15} = 3.82$, $^*P = 0.006$), travel longer distances in the open arms (middle; $t_{10} = 3.59$, $^*P = 0.015$) and spend more time in the open arms (right; $t_{15} = 9.73$, $^*P = 0.006$) of the elevated plus maze compared to control mice. Data presented as mean ± s.e.m.; $n = 7$ (control) and 10 (*CRFR1*$^{PVN\text{-}cKO}$) mice per group.

the Adelis Foundation and the Irving I. Moskowitz Foundation; the I-CORE Program of the Planning and Budgeting Committee; and the Israel Science Foundation (grant No 1916/12). Y.K. is supported by Sarah and Rolando Uziel.

AUTHOR CONTRIBUTIONS

A.R. designed and performed most of the experiments. Z.J., J.-B.T. and N.J. designed and performed electrophysiological studies. Z.J. and N.J. performed the single-cell reverse-transcription-PCR. Y.K. and T.N. assisted in experiments. A.R., N.J. and A.C. conceived, designed and supervised the project. A.R., N.J. and A.C. wrote the manuscript.

COMPETING FINANCIAL INTERESTS

The authors declare no competing financial interests.

1. Ulrich-Lai, Y.M. & Herman, J.P. *Nat. Rev. Neurosci.* **10**, 397–409 (2009).
2. Raison, C.L. & Miller, A.H. *Am. J. Psychiatry* **160**, 1554–1565 (2003).
3. de Kloet, C.S. *et al. J. Psychiatr. Res.* **40**, 550–567 (2006).
4. Vale, W., Spiess, J., Rivier, C. & Rivier, J. *Science* **213**, 1394–1397 (1981).
5. Rivier, C. & Vale, W. *Nature* **305**, 325–327 (1983).
6. Dallman, M.F., Akana, S.F., Bhatnagar, S., Bell, M.E. & Strack, A.M. *Int. J. Obes.* **24** (Suppl. 2), S40–S46 (2000).
7. De Kloet, E.R., Vreugdenhil, E., Oitzl, M.S. & Joëls, M. *Endocr. Rev.* **19**, 269–301 (1998).
8. Chen, R., Lewis, K.A., Perrin, M.H. & Vale, W.W. *Proc. Natl. Acad. Sci. USA* **90**, 8967–8971 (1993).
9. Lovenberg, T.W. *et al. Proc. Natl. Acad. Sci. USA* **92**, 836–840 (1995).
10. Justice, N.J., Yuan, Z.F., Sawchenko, P.E. & Vale, W. *J. Comp. Neurol.* **511**, 479–496 (2008).
11. Van Pett, K. *et al. J. Comp. Neurol.* **428**, 191–212 (2000).
12. Henckens, M.J.A.G., Deussing, J.M. & Chen, A. *Nat. Rev. Neurosci.* **17**, 636–651 (2016).
13. Refojo, D. *et al. Science* **333**, 1903–1907 (2011).
14. Gulyas, J. *et al. Proc. Natl. Acad. Sci. USA* **92**, 10575–10579 (1995).
15. Taniguchi, H. *et al. Neuron* **71**, 995–1013 (2011).
16. Smith, G.W. *et al. Neuron* **20**, 1093–1102 (1998).
17. Balthasar, N. *et al. Cell* **123**, 493–505 (2005).
18. Madisen, L. *et al. Nat. Neurosci.* **13**, 133–140 (2010).
19. Krishnan, V. *et al. Cell* **131**, 391–404 (2007).
20. Wang, S.-S., Kamphuis, W., Huitinga, I., Zhou, J.-N. & Swaab, D.F. *Mol. Psychiatry* **13**, 786–799, 741 (2008).

ONLINE METHODS

Animals and animal care. Mice (males, C57BL/6, 2–5 months old) were maintained in a pathogen-free temperature-controlled (22 °C ± 1) mouse facility on a reverse-phase 12-h light-dark cycle at the Weizmann Institute of Science, according to institutional guidelines. Food and water were given *ad libitum*. No more than 5 mice were housed per cage. All experimental protocols were approved by the Institutional Animal Care and Use Committee of The Weizmann Institute of Science. Littermates were randomly divided into different groups (except for experiments conducted on mice with specific genotypes). All behavioral tests were carried out during the dark phase.

Immunohistological analysis. Animals were anesthetized and transcardially perfused with 4% paraformaldehyde (PFA). Brains were postfixed with 30% sucrose solution in 4% PFA. Fixed brains were serially sectioned (30–50 µm). Sections were incubated in blocking solution (20% horse serum, 0.2% Triton in PBS) for 2 h to prevent nonspecific binding of antibodies. Sections were then incubated overnight with the primary antibody in PBS containing 2% horse serum and 0.2% triton. Following PBS washes, sections were incubated for 1–1.5 h at room temperature with the appropriate secondary antibodies (Jackson ImmunoResearch Laboratories Inc., West Grove, PA, USA). Sections were washed with PBS and then mounted on slides. Images were captured using a confocal microscope (Zeiss LSM700). Cells were counted and their somatal volume measured using Imaris software (spot detection and surface modules, respectively; version 8.02; Bitplane). The following primary antibodies were used: anti-GFP (1:250; #ab6556, Abcam, Cambridge, UK), anti-c-Fos (1:1,000; #sc52, Santa Cruz Biotechnology Inc., Dallas, TX, USA), anti-CRF (1:2,000; kindly provided by Dr. Wylie Vale, The Salk Institute), anti-oxytocin (1:1,000; #t5021, Peninsula Laboratories, CA, USA), anti-AVP (1:1,000; #t5048, Peninsula Laboratories, CA, USA) and anti-GR (1:1,000, #sc1004, Santa Cruz Biotechnology Inc., Dallas, TX, USA). To identify PVN neurosecretory neurons, mice received intravenous injections of 20 µl 2% Fluoro-Gold (Fluorochrome, Denver, CO, USA). The following secondary antibodies were used: anti-rabbit Alexa Fluor 594 (1:200; A-21207, Life Technologies, Paisley, UK), anti-rabbit Alexa Fluor 488 (1:200; A-21206, Life Technologies, Paisley, UK), anti-rabbit Alexa Fluor 647 (1:200; A-31573, Life Technologies, Paisley, UK) and anti-guinea pig Cy5 (1:200; Jackson ImmunoResearch, West Grove, PA, USA).

Stereotaxic injections. Mice aged 2–4 months were anaesthetized with 1.5% isoflurane (Abbott, Abbott Park, IL, USA) and placed in a computer-guided stereotaxic instrument (Angle Two Stereotaxic Instrument, myNeurolab, Leica Microsystems Inc., Bannockburn, IL, USA). For immunostaining of CRF (**Fig. 1a**), mice were injected with colchicine (2 µl of 1 µg/µl dilution) into the lateral ventricles (AP −0.20 mm; ML +0.95 mm; DV −2.2 mm). Mice were killed by perfusion when locomotor symptoms were observed (3–4 days following colchicine injection). For observation of synapses originating from PVN CRF$^+$ neurons, 300 nl of virus encoding Cre-dependent mCherry ($AAV_{1,2}$-DIO-mCherry viral vector, courtesy of Dr. Ofer Yizhar) was injected unilaterally into the PVN of $CRF^{Cre} \times CRFR1^{GFP}$ mice (AP −0.9 mm; ML +0.25 mm; DV −4.7 mm). For optogenetic activation of PVN CRF$^+$ neurons, 150 nl of virus encoding Cre-dependent ChR2-mRuby (AAV-EF1a-DIO-hChR2(H134R)-p2A-Ruby, kindly provided by Dr. Benjamin Arenkiel) was injected bilaterally into the PVN of $CRF^{Cre} \times CRFR1^{GFP}$ mice (AP −0.2 mm; ML ±0.2 mm; DV −4.8 mm). Mice were allowed to recover for at least 3 weeks before being used in experiments.

Adrenalectomy (ADX). ADX was performed through a dorsal incision under ketamine/xylazine anesthesia (1 ml ketamine + 1 ml xylazine + 8 ml saline; 0.1 ml cocktail per 10 g body weight). Animals were excluded if their CORT levels following ADX remained similar to the level prior the surgery, under the assumption that this indicated the adrenal glands were not completely removed.

Acute stress exposure. For restraint stress, mice were subjected to 15 min in a ventilated, 50 ml plastic centrifuge tube and then returned to the home cage. For hemorrhage stress, a fine-walled Pasteur pipette was inserted into the corner of the eye socket underneath the eyeball, and 200 µl of blood were taken. Immune stress was induced by i.p. injection of LPS (100 µg, from *E. coli*, Sigma-Aldrich, Wicklow, Ireland). For the DEX suppression test, DEX (10 µg/100 g mouse body weight) or saline was injected i.p. to mice 2 h before blood was sampled.

Corticosterone measurements. Plasma was extracted from blood samples that were collected by tail bleed under basal conditions and at different time points following and/or during different stress exposures. Blood samples were centrifuged (3,500 rpm for 25 min at 4 °C) and extracted plasma was stored at −80 °C until assayed for CORT using a radioimmunoassay kit (ImmuChem^{TM} Double Antibody Corticosterone ^{125}I RIA KIT, MP Biomedicals, NY, USA).

Slice electrophysiology. CRFR1-GFP mice (8–12 weeks old) were anesthetized by isoflurane and decapitated. The brain was quickly excised and immersed in ice-cold cutting solution consisting of (in mM): 60 NaCl, 110 sucrose, 28 $NaHCO_3$, 7 $MgSO_4$, 3 KCl, 1.25 NaH_2PO_4, 0.5 $CaCl_2$ and 0.6 sodium ascorbate, bubbled with 95% O_2 + 5% CO_2, until the brain tissue was chilled completely. Subsequently, 250-µm coronal slices containing the PVN were obtained using a Leica VT1200S vibratome (Leica Microsystems, Wetzlar, Germany). Slices were immediately transferred and incubated in normal artificial cerebrospinal fluid (aCSF) consisting of (in mM): 125 NaCl, 26 $NaHCO_3$, 1 $MgSO_4$, 2.5 KCl, 1.25 NaH_2PO_4, 2 $CaCl_2$ and 10 glucose, bubbled with 95% O_2 + 5% CO_2, at 35 °C for at least 60 min before recording. Individual brain slices were placed in the recording chamber (Warner Instruments, Hamden, CT, USA) and continuously perfused with either normal aCSF or modified aCSF supplemented with 20 µM CNQX, 30 µM D-AP5 and 100 µM picrotoxin to block fast synaptic transmission mediated by AMPA, NMDA and $GABA_A$ receptors, respectively. CRF was diluted in either normal or modified aCSF, as indicated in the results, and applied through whole-chamber perfusion. Glass pipettes (Sutter Instrument, Novalto, CA, USA) were pulled using a Narishige PC-10 puller. The pipette tip resistance was 3–5 MΩ when filled with the intracellular solution containing (in mM): 122 potassium gluconate, 9 NaCl, 1.8 $MgCl_2$, 0.9 EGTA, 9 HEPES, 14 Tris-creatine-PO_4, 4 Mg-ATP and 0.3 Tris-GTP, with pH adjusted to 7.4 by KOH and osmolarity of 300 mOsm. CRF$^+$ PVN neurons were visualized using a 60× water objective lens and infrared-differential interference contrast/fluorescence videomicroscopy (Olympus BX51WI with OLY-150IR video camera; Olympus Deutschland GmbH, Hamburg, Germany). Selected PVN neurons were voltage clamped at −70 mV before switching to current-clamp mode, and current was injected to allow action potential firing at low frequency. Cell firing was continuously monitored and recorded before and during drug administration. The temperature of the recording chamber was maintained at approximately 32 °C by passing the perfusion solution through an inline heater (Warner Instruments, Hamden, CT, USA) at 3 ml/min, driven by a Rabbit peristaltic pump (Mettler-Toledo Rainin, Oakland, CA, USA). Data were acquired using an EPC10 amplifier operated by PatchMaster software (both from Heka Elektronik, Lambrecht, Germany). Recordings were filtered at 3 kHz and digitized at 10 kHz. Firing frequency was calculated as spikes per second. All measurements were made offline using the analysis functions of the PatchMaster software. Representative traces in figures were reproduced in OriginPro (OriginLab, Northampton, MA, USA). For optical activation of CRF$^+$ neurons, 1–3 min laser trains (473 nm, 1 Hz, 5 ms, 5–6 mW, PSU-III-LED laser system; Optoengine, Midvale, UT, USA) were delivered via an optical fiber placed close to the recording site.

Single-cell RT-PCR for molecular phenotyping. Cell contents of PVN CRFR1-GFP$^+$ neurons were aspirated into glass pipettes filled with RNAse-free internal solution, and the tip of each pipette containing the cell contents was broken into an RNAse-free PCR tube containing 1 µl RNAse inhibitor (rRNAsin, Promega, Madison, WI, USA) and 2 µl RNAse-free water on dry ice. Tubes containing single-cell contents were stored at −80 °C before further processing.

For single-cell RT-PCR, cDNA was made from RNA isolated from single cells using the ProtoScript II First Strand cDNA Synthesis Kit (E6560S/L, New England BioLabs, Ipswich, MA, USA). Multiplex PCR was carried out with an outside primers mix (**Supplementary Table 1**) using the previously generated cDNA samples in a volume of 50 µl for 50 cycles. A nested single-gene PCR was then performed in a volume of 20 µl using 1 µl of the multiplex cDNA as a template (Apex 2X Taq RED master mix, Genesee Scientific, San Diego, CA, USA). PCR products were visualized and documented with standard agarose gel electrophoresis (**Supplementary Table 1**). PCR products were sequenced to check for nonspecific amplification. We included negative control reactions with no added template in each experiment; amplification of *Gapdh* mRNA served as an internal positive control. Data were only included

from experiments in which there were positive signals from internal positive controls and no contamination in the negative control.

General locomotion. Locomotion was assessed using the InfraMot system (TSE-Systems, Bad Homburg, Germany). Mice were housed individually in the system cages for a period of 72 h; data were collected at 1-h intervals.

Open field test (OFT). The apparatus (TSE-systems, Bad Homburg, Germany) consists of a white Plexiglas box (50 cm × 50 cm × height 40 cm), brightly illuminated (120 lx). This test takes advantage of the natural conflict within a rodent between the desire to explore a novel environment and the aversive properties of a large, brightly lit area. Each mouse was placed in the corner of the apparatus to initiate a 10-min test session. A camera (Eneo, Rödermark, Germany; Model: VK1316S) mounted above the apparatus transmitted images of the mice, which were analyzed by TSE-systems' VideoMot2 software. The following indices were recorded and subsequently analyzed: time spent in the center; number of visits to the center and total distance traveled. More frequent or longer times spent exploring the arena or in the center of the arena are seen as less anxiety-like behaviors.

Elevated-plus maze (EPM). The EPM test was carried out at least 2 d following the OFT. The EPM apparatus comprises a central part (5 × 5 cm), two opposing open arms (30.5 × 5 cm) and two opposing closed arms (30.5 × 5 × 15 cm). The apparatus was elevated at a height of 53.5 cm and the open arms were illuminated at 6 lx. Mice were placed in the center, facing an open arm, to initiate a 5-min session test. The time spent and distance travelled in the open or closed arms and the number of entries into the open or closed arms were measured.

Chronic social defeat stress (CSDS). CSDS is a well-established protocol for the induction of prolonged anxiety-like behavior in rodents[19]. Adult mice were subjected to the social defeat protocol. Briefly, the mice were placed in the home cage of an aggressive ICR mouse, where they physically interacted for 5 min. During this time, the ICR mouse attacked the intruder mouse and the intruder displayed subordinate posturing. A perforated, clear Plexiglass divider was then placed between the animals and they remained in the same cage for 24 h to allow sensory contact. The procedure was then repeated with an unfamiliar ICR mouse for each of the next 10 d.

Statistical analysis. Results are expressed as mean ± s.e.m. Data collection and analyses were not performed blind to the conditions of the experiments, except for corticosterone measurements and behavioral tests. Automated analysis was used whenever possible, including cell counting and behavioral measurements. No statistical methods were used to predetermine sample sizes, but our sample sizes are similar to those reported in previous publications[21]. Statistical analysis was performed using Student's *t*-tests or repeated-measures ANOVA with *post hoc* Student's *t*-tests (one-way ANOVA) where appropriate. All statistical tests were two-sided. Data were tested for normality. Levene's test was used to assess the equality of variances between the groups. Bonferroni corrections for multiple comparisons were performed when needed. Any samples that were 2 s.d. above or below the mean were excluded. Analyses were performed using SPSS 16.0 (SPSS Inc., Chicago, IL, USA). A **Supplementary Methods Checklist** is available.

Data availability statement. The data that support the findings of this study are available from the corresponding author upon reasonable request.

21. Henckens, M.J.A.G. *et al. Mol. Psychiatry* http://www.nature.com/mp/journal/vaop/ncurrent/full/mp2016133a.html (2016).

doi:10.1038/nn.4491